

Short Communication

# Natural frequencies of an orthotropic thin toroidal shell of elliptical cross-section

B. Xu, D. Redekop\*

*Department of Mechanical Engineering, University of Ottawa, Ottawa, Canada K1N 6N5*

Received 7 September 2005; received in revised form 7 September 2005; accepted 18 September 2005

Available online 9 November 2005

---

## Abstract

A method is presented to determine the natural frequencies of an orthotropic thin toroidal shell of elliptical cross-section. The solution is based on the classical Sanders–Budiansky shell theory and uses the differential quadrature method (DQM) to obtain numerical results. The appropriate scheme for the selection of the sampling points in the DQM for shells of elliptical cross-section is indicated. Values for frequencies are given for complete toroidal shells, which are entirely free of supports, or with a support along a circumferential line. The results obtained from the method show close agreement with previously published results, and with results obtained using the finite element method.

© 2005 Elsevier Ltd. All rights reserved.

---

## 1. Introduction

Toroidal shells have been proposed for, or used, in such applications as fusion reactor vessels, satellite antenna support structures, protective devices for nuclear fuel containers, circumferential reinforcement for submarines, rocket fuel tanks, and diver's oxygen tanks. The literature on the vibration of toroidal shells includes work dealing mainly with isotropic shells of circular cross-section. Yamada et al. [1] considered isotropic toroidal shells with elliptical cross-section. Wang and Redekop [2] considered orthotropic toroidal shells with circular cross-section. There is little work, if any, on orthotropic toroidal shells of elliptical cross-section.

In the present work, the theory developed by Wang and Redekop [2] is modified to cover the case of orthotropic toroidal shells with elliptical cross-section. A scheme is specified for the selection of the differential quadrature method (DQM) sampling points for this type of geometry. Results from the approach are first compared with the results of Yamada et al. [1] for isotropic shells of elliptical cross-sections. Further comparisons are made with the results of Wang and Redekop [2] for orthotropic shells of circular cross-section. New DQM results are then found for completely free orthotropic shells of prolate and oblate elliptical cross-section, and for isotropic prolate elliptical shells with a line support on the inner equatorial line. FEM results are also presented for comparison purposes, and these show good agreement with the DQM results.

---

\*Corresponding author. Tel.: +1 613 562 5800x6290; fax: +1 613 562 5177.

E-mail address: [dredkop@uottawa.ca](mailto:dredkop@uottawa.ca) (D. Redekop).

### 2. Shell theory

The theory is developed for a toroidal shell of elliptical cross-section (Fig. 1) with bend radius  $R$ , axis in the  $z$  direction  $2a$ , axis in radial direction  $2b$ , and wall thickness  $h$ . The circumferential coordinate about  $z$  is  $q_1 \equiv \phi$  and the meridional coordinate  $q_2 \equiv \psi$ . The radius vector is given by

$$\mathbf{R} = r \sin \phi \mathbf{i} + r \cos \phi \mathbf{j} + z \mathbf{k}, \tag{1}$$

where  $r = R + (b^2/G) \sin \psi$ ,  $z = (a^2/G) \cos \psi$ , and  $G = \sqrt{a^2 \cos^2 \psi + b^2 \sin^2 \psi}$ . The Lamé parameters  $\alpha_i$  and curvatures  $k_i$  are then given by [3]

$$\alpha_1 = r; \quad \alpha_2 = a^2 b^2 / G^3; \quad k_1 = \sin \psi / r; \quad k_2 = G^3 / (a^2 b^2). \tag{2}$$

Assuming harmonic motion, the displacement components for the  $m$ th mode are taken as

$$\begin{aligned} u_1 &= u(q_2) \sin m\phi \sin \omega t, \\ u_2 &= v(q_2) \cos m\phi \sin \omega t, \\ u_3 &= w(q_2) \cos m\phi \sin \omega t, \end{aligned} \tag{3}$$

where  $u, v, w$  represent the displacement functions in the circumferential, meridional, and normal directions, dependent on the meridional coordinate  $q_2$  only,  $\omega$  is the natural frequency, and  $t$  is the time. Application of the modal expressions (3) leads to a one-dimensional mathematical problem [2], and effectively permits the analysis of a typical cross-section of the shell. The displacement components (3) are substituted into the governing equations for an orthotropic thin shell of revolution [2], and the equations are simplified to the following field conditions for the displacement functions:

$$\begin{aligned} e_1 u_{,22} + e_2 u_{,1} + (e_3 + m^2 e_4) u + m e_5 v_{,2} + m e_6 v + m e_7 w_{,22} + m e_8 w_{,2} \\ + (m^3 e_9 + m e_{10}) w = \Omega u, \end{aligned}$$

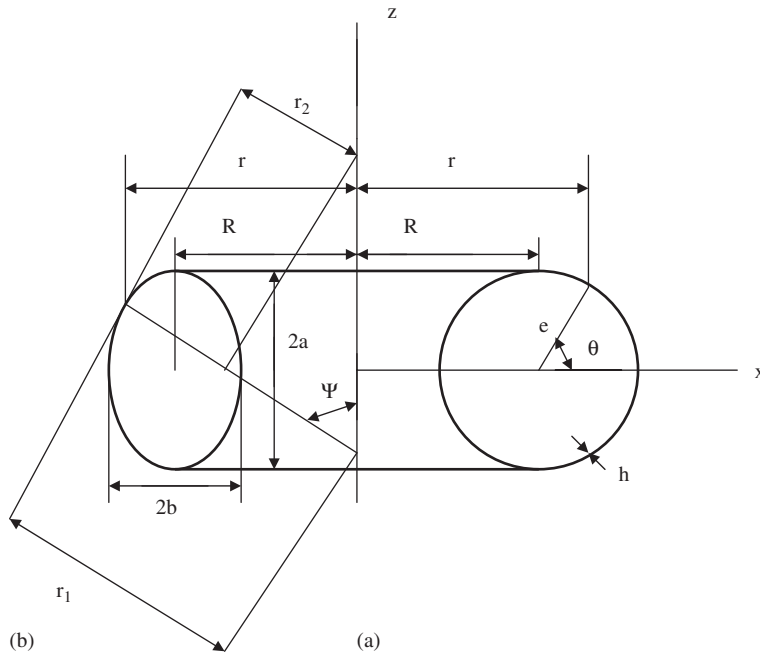


Fig. 1. Cross-sectional geometry of toroidal shell (a) circular and (b) elliptical.

$$\begin{aligned}
& me_{11}u_{,2} + me_{12}u + e_{13}v_{,22} + me_{14}v_{,2} + (e_{15} + m^2e_{16})v + me_{17}w_{,222} + me_{18}w_{,22} \\
& + (e_{19} + e_{20}m^2)w_{,2} + (e_{21} + m^2e_{22})w = \Omega v, \\
& me_{23}u_{,22} + me_{24}u_{,2} + (m^3e_{25} + me_{26})u + e_{27}v_{,222} + e_{28}v_{,22} + (e_{29} + m^2e_{30})v_{,2} \\
& + (m^2e_{31} + e_{32})v + e_{33}w_{,2222} + e_{34}w_{,222} + (e_{35} + m^2e_{36})w_{,22} + (e_{37} + m^2e_{38})w_{,2} \\
& + (e_{39} + m^2e_{40} + m^4e_{41})w = \Omega w.
\end{aligned} \tag{4}$$

In Eq. (4) the  $e_i$ ,  $i = 1, \dots, 41$  are known functions of the Lamé parameters and curvatures, and the material properties,  $\Omega = \rho h \omega^2$ , and  $\rho$  is the mass density [2]. The comma subscript in Eq. (4) indicates differentiation with respect to the meridional coordinate. In this shell theory, for orthotropic materials, the independent material properties include two Young's moduli, a shear modulus, and a Poisson's ratio. The set of ordinary differential equations (4) contains as the unknowns the displacement functions and the natural frequency parameter  $\Omega$  of the  $m$ th harmonic. The  $m = 0$  case, i.e. the axisymmetric circumferential harmonic, is a special case which can easily be extracted from the general theory.

For a complete toroidal shell the meridian forms a closed curve, and boundary conditions need not be considered. In the present study shells with a circumferential line constraint are also considered. For those shells the governing equations are replaced by the restraint conditions

$$u = v = w = 0 \tag{5}$$

at the point on the cross-section representing the line of constraint.

### 3. Differential quadrature method

In the DQM [4] a grid of sampling points covering the domain, including the boundary must first be defined. For the present geometry a set of sampling points following a typical meridian is required. The replacement of all derivatives with series of terms that contain the product of the displacement functions at the sampling points and the weighting coefficients must next be made. This second step converts the problem from one of differential equations to one of linear algebraic equations. The  $r$ th derivative of a generic function of a single variable  $f(x)$  at the sampling point  $x_i$  is replaced by the series

$$\left. \frac{d^r f(x)}{dx^r} \right|_{x_i} = \sum_{h=1}^M A_{ih}^{(r)} f(x_h), \tag{6}$$

where the  $A_{ih}^{(r)}$  are the weighting coefficients of the  $r$ th-order derivative in the  $x$  direction for the  $i$ th sampling point,  $f(x_h)$  is the value of  $f(x)$  at the sampling point position  $x_h$ , and  $M$  is the number of sampling points in the  $x$  direction.

In the DQM the weighting coefficients are determined a priori for a preselected grid, with the aid of selected trial functions. For the present geometry involving a complete meridian, it is convenient to use a Fourier harmonic basis for the weighting coefficients, and to use equally spaced points in the coordinate of this direction  $\psi$ . It is evident that the points will not be equally spaced geodetically around the meridian. For such a scheme, explicit formulas for the weighting coefficients  $A_{ih}^{(r)}$  are available [4].

Use of the quadrature rule (6) for the derivatives in the field equations (4) leads to transformed algebraic DQM vibration equations. Enforcement of these equations at the sampling points leads to the set of equations

$$[K](U) = \beta[M](U), \tag{7}$$

where the unknowns ( $U$ ) are the values of the displacement functions at the sampling points,  $\beta$  is the unknown eigenvalue, related to  $\omega$ , and  $[K]$ ,  $[M]$  are the known 'stiffness' and 'mass' matrices. For the geometry involving line support of the shell, the field equations corresponding to the sampling point at the support are replaced by the restraint conditions (5) prior to the formation of Eq. (7).

4. Finite element method

The commercial FEM program ADINA [5] is used to provide an alternate solution to the vibration problem. A four-noded 24 degree-of-freedom shear–deformation shell element is used for the analysis. Selections in meshing options are made to give elements that are nearly square in plan at the equator. The modeling accounts for the full geometry, with no account made of any symmetry. The eigenvalues were found using both the subspace iteration and Lanczos method. The numerical values produced by the two methods were virtually identical, but the speed of the Lanczos method was much greater.

5. Validation and results

Two examples involving completely free toroidal shells are presented to validate the current method. The first is for an isotropic elliptical toroidal shell, and the second is for an orthotropic circular toroidal shell (Fig. 1a). In Table 1 comparisons for the frequency parameter  $\lambda$  [1] are given for the first example. The comparisons are made first with the transfer matrix approach (TMA) of Yamada et al. [1], and then with the FEM. Indicated also in the first comparison are the convergence characteristics of the DQM approach. The ellipses are of the prolate (major axis along the  $z$ -axis), and of the oblate (major axis along the  $r$ -axis) forms. Both

Table 1  
Comparison of  $\lambda$  for isotropic elliptical toroidal shells with Yamada et al. [1] and with FEM

Method	$\lambda_1$	$\lambda_2$	$\lambda_3$	$\lambda_4$	$\lambda_5$	$\lambda_6$	$\lambda_7$	$\lambda_8$
<i>Prolate (m = 2)</i>								
DQM(20)	0.02220	0.02344	0.2019	0.2155	0.2672	0.2681	0.2851	0.2911
DQM(40)	0.02231	0.02356	0.2020	0.2669	0.2678	0.2828	0.2920	0.2973
DQM(60)	0.02231	0.02356	0.2020	0.2669	0.2678	0.2828	0.2920	0.2973
DQM(100)	0.02231	0.02356	0.2020	0.2669	0.2678	0.2828	0.2920	0.2973
TMA [1]	0.02217	0.02750	0.2021	0.2660	0.2686	0.2832	0.2917	0.2974
<i>Oblate (m = 2)</i>								
DQM(20)	0.04108	0.08420	0.11103	0.12929	0.1460	0.1657	0.1708	0.2238
DQM(40)	0.02979	0.03090	0.08846	0.09113	0.1135	0.1173	0.1204	0.1444
DQM(60)	0.02982	0.03090	0.08890	0.08994	0.1140	0.1152	0.1239	0.1429
DQM(100)	0.02982	0.03090	0.08891	0.08994	0.1140	0.1152	0.1240	0.1428
TMA [1]	0.02975	0.03215	0.08877	0.08979	0.1142	0.1151	0.1242	0.1429
<i>Prolate (all m)</i>								
DQM(100)	0.01006	0.02231	0.02356	0.04323	0.0442	0.0579	0.0601	0.0734
FEM	—	0.02220	0.02751	0.03896	0.0437	0.0453	0.0596	0.0744
<i>Oblate (all m)</i>								
DQM(100)	0.01030	0.02982	0.03090	0.04884	0.0507	0.0736	0.0742	0.0872
FEM	0.01494	0.02966	0.03201	0.04985	0.0502	0.0741	0.0747	0.0870

Table 2  
Geometry of circular and elliptical toroidal shell cases ( $R = 1$  m)

Case	1—Circular				2—Prolate		3—Oblate	
	$e(m)$	$h(m)$	$R/e$	$e/h$	$a(m)$	$b(m)$	$a(m)$	$b(m)$
A	0.25	0.0025	4	100	0.3	0.2	0.2	0.3
B	0.25	0.0050	4	50	0.3	0.2	0.2	0.3
C	0.50	0.0050	2	100	0.6	0.4	0.4	0.6
D	0.75	0.0075	4/3	100	0.8	0.7	0.7	0.8

ellipses have the following geometric properties:  $R = 0.3855$  m,  $h = 0.001542$  m, semi-major axis 0.2 m, and semi-minor axis of 0.1 m. The values for the material properties were taken as

$$E = 200 \text{ GPa}; \quad \nu = 0.3; \quad \rho = 7800 \text{ kg/m}^3. \tag{8}$$

The TMA results are for the second circumferential harmonic ( $m = 2$ ), and are taken from the quoted values given in Fig. 3 of Yamada et al. [1]. There is agreement within 1% for all eigenvalues, except the second one, for both the prolate and oblate forms. Comparisons made with the FEM results cover all harmonics. There is generally good agreement in the two sets of results for both the prolate and the oblate forms.

A description of four cases of toroidal shell geometries (A, B, C, D) is given in Table 2. These geometries were considered earlier in Ref. [2] for circular cross-sections. Four variations of these geometries (1, 2, 3, 4) are considered in this work. In the first three variations completely free support conditions and an orthotropic

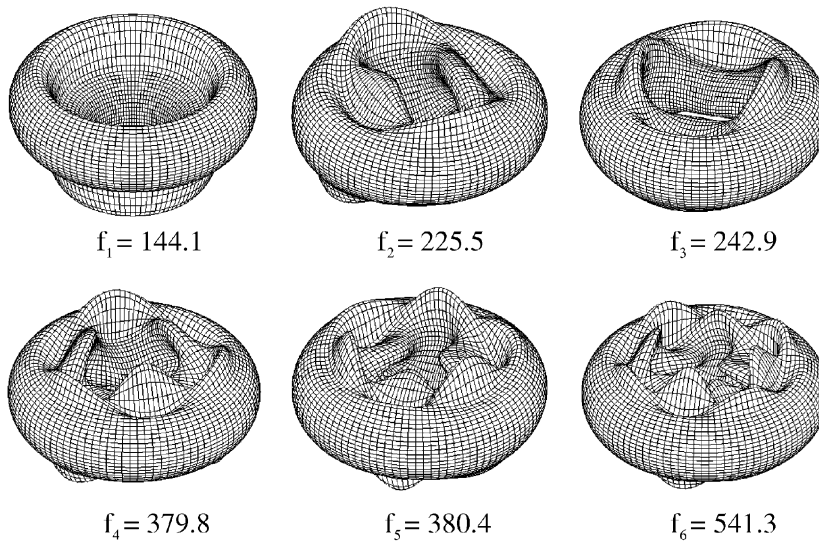


Fig. 2. Mode shapes 1–6 for circular toroidal shell C1 (frequencies in rad/s).

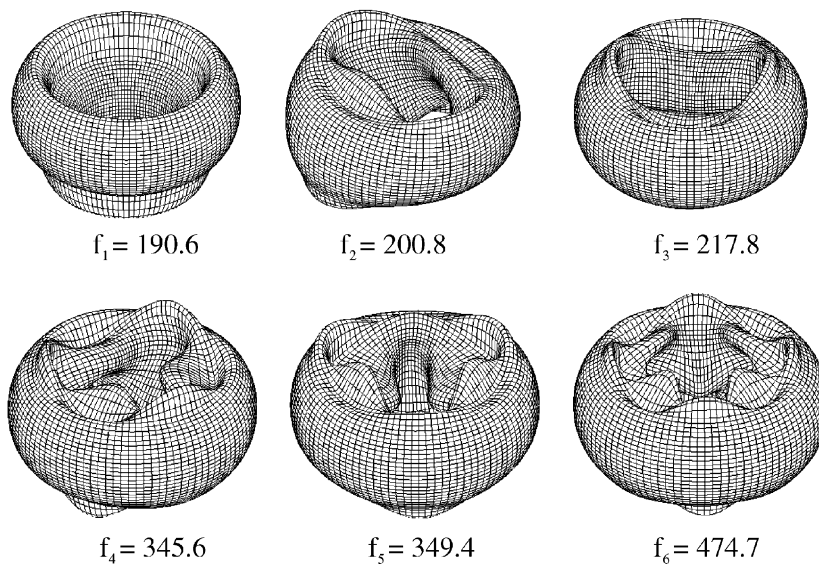


Fig. 3. Mode shapes 1–6 for prolate elliptical toroidal shell C2 (frequencies in rad/s).



material are assumed, while in the last one a line support at the inner equator and an isotropic material are assumed. The cross-sections in the four variations are, respectively, circular, prolate elliptical, oblate elliptical, and prolate elliptical. The second and fourth variations are thus identical geometrically, aside from the support. The values for the orthotropic material were taken as

$$E_1 = 7.44 \text{ GPa}; \quad E_2 = 3.47 \text{ GPa}; \quad G_{12} = 2.04 \text{ GPa}; \quad \nu_{12} = 0.149; \quad \rho = 700 \text{ kg/m}^3. \quad (9)$$

This material is stiffer in the circumferential direction than in the meridional direction.

In Table 3, a comparison is given of the DQM and FEM results for the natural frequencies of the shell cases A1, B1, C1 and D1 of Table 2, i.e. for the circular cross-section. Also given are the DQM values for  $m$  that indicate the circumferential harmonic. For the DQM two sets of results are given; the first stemming from an analysis considering the cross-section as a circle [2] (DQM-cir), the second stemming from an analysis considering the cross-section as an ellipse with equal axes (DQM-ell). The results from the first analysis are the same as those reported in the study [2] aside from a value containing a typographical error (marked with a

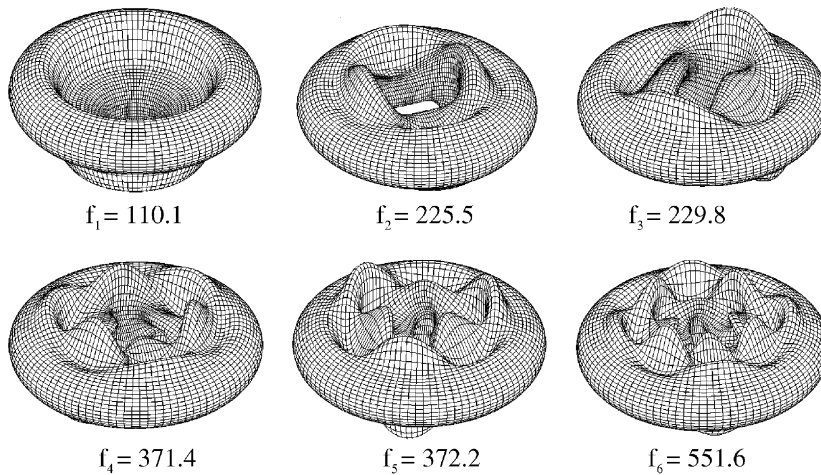


Fig. 4. Mode shapes 1–6 for oblate elliptical toroidal shell C3 (frequencies in rad/s).

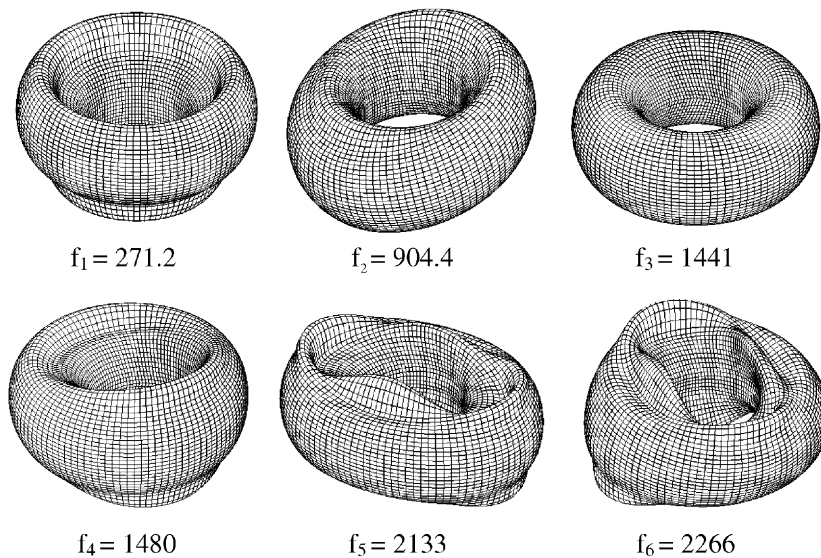


Fig. 5. Mode shapes 1–6 for isotropic prolate elliptical toroidal shell C4 with inner equator line support (frequencies in rad/s).

asterisk). The results from the two DQM analysis agree to four figures. The differences between the DQM and FEM results range from 0.6% to 8.6%.

New results for natural frequencies are given in Tables 4 and 5 for the variations 2 and 3 of the four basic toroidal geometries of Table 2, for the orthotropic material defined in (9). The  $m$  values of the tables represent the circumferential harmonic as given by the DQM. In Table 4 the DQM results for the completely free toroidal shells of prolate elliptical cross-section show differences with FEM results ranging from 0.1% to 10.5%. In Table 5, the DQM results for completely free toroidal shells of oblate elliptical cross-section show differences with FEM results ranging from 0.4% to 9.8%. Comparing corresponding values of the two tables it is seen that for the A and B geometries the fundamental frequencies are comparable, whereas for the C and D geometries the fundamental frequencies of the prolate shells are significantly higher. Comparing corresponding values of Table 3 with those of Tables 4 and 5 it seen that the shells with circular

Table 3  
Comparison of  $\omega$  (rad/s) for orthotropic circular toroidal shells (C1 modes shown in Fig. 2)

Case	Method	$\omega_1$	$\omega_2$	$\omega_3$	$\omega_4$	$\omega_5$	$\omega_6$
A1	$m$	2	2	0	3	3	4
	FEM	187.5	192.3	197.5	335.4	339.3	454.2
	DQM-cir	186.2	191.2	199.7	330.4	334.3	442.2
	DQM-ell	186.2	191.2	199.7	330.4	334.3	442.2
B1	$m$	2	2	0	3	3	4
	FEM	267.4	274.7	283.5	496.1	502.5	694.5
	DQM-cir	263.4	271.3*	287.5	485.1	491.7	670.7
	DQM-ell	263.4	271.3	287.5	485.1	491.7	670.7
C1	$m$	0	2	2	3	3	—
	FEM	144.1	225.5	242.9	379.8	380.4	541.3
	DQM-cir	146.0	220.4	238.0	364.0	364.8	—
	DQM-ell	146.0	220.4	238.0	364.0	364.8	—
D1	$m$	0	2	2	2	1	2
	FEM	126.7	278.9	292.7	525.4	525.6	594.8
	DQM-cir	129.1	269.6	284.2	529.4	542.8	546.1
	DQM-ell	129.1	269.6	284.2	529.4	542.8	546.1

(for the entry \* in the B1 values a typographical error appears in Ref. [2]).

Table 4  
Results for  $\omega$  (rad/s) for orthotropic prolate elliptical toroidal shells (C2 modes shown in Fig. 3)

Case	Method	$\omega_1$	$\omega_2$	$\omega_3$	$\omega_4$	$\omega_5$	$\omega_6$
A2	$m$	2	2	0	3	3	4
	FEM	146.8	185.2	263.6	311.5	322.4	423.1
	DQM	148.6	178.4	264.2	311.2	314.9	413.0
B2	$m$	2	2	0	3	3	4
	FEM	207.1	260.9	374.9	446.6	464.3	621.4
	DQM	209.1	243.0	372.6	443.6	449.4	602.5
C2	$m$	0	2	2	3	3	4
	FEM	190.6	200.8	217.8	345.6	349.4	474.7
	DQM	192.3	195.7	217.5	335.6	337.3	451.4
D2	$m$	0	2	2	2	2	1
	FEM	137.9	270.3	281.0	503.0	647.4	664.5
	DQM	139.7	261.8	273.0	558.6	617.2	628.7

Table 5  
Results for  $\omega$  (rad/s) for orthotropic oblate elliptical toroidal shells (C3 modes shown in Fig. 4)

Case	Method	$\omega_1$	$\omega_2$	$\omega_3$	$\omega_4$	$\omega_5$	$\omega_6$
A3	<i>m</i>	0	2	2	3	3	4
	FEM	149.3	186.1	206.3	317.4	324.9	439.8
	QM	144.3	177.3	208.7	313.2	313.6	424.8
B3	<i>m</i>	0	2	2	3	3	4
	FEM	215.8	269.0	302.0	484.3	497.9	698.5
	DQM	198.2	244.0	309.6	470.7	478.2	667.9
C3	<i>m</i>	0	2	2	3	3	—
	FEM	110.1	225.5	229.8	371.4	372.2	551.6
	DQM	109.7	220.4	222.4	354.0	354.8	—
D3	<i>m</i>	0	2	2	1	—	—
	FEM	117.2	288.4	296.4	480.3	498.6	503.0
	DQM	119.7	280.0	288.1	453.0	—	—

Table 6  
Results for  $\omega$  (rad/s) for isotropic prolate elliptical toroidal shells with inner equator line support (C4 modes shown in Fig. 5)

Case	Method	$\omega_1$	$\omega_2$	$\omega_3$	$\omega_4$	$\omega_5$	$\omega_6$
A4	<i>m</i>	0	1	2	1	2	5
	FEM	332.0	1306	3079	3180	3283	3394
	DQM	327.3	1284	3027	3135	3232	3349
B4	<i>m</i>	0	1	2	1	2	0
	FEM	472.9	1340	3097	3229	3365	3785
	DQM	465.6	1321	3050	3188	3315	3722
C4	<i>m</i>	0	1	—	1	2	2
	FEM	271.2	904.4	1441	1480	2133	2266
	DQM	217.5	906.0	—	1486	2131	2270
D4	<i>m</i>	0	—	1	1	2	2
	FEM	134.7	385.1	405.0	586.6	1323	1338
	DQM	134.6	—	407.7	587.6	1328	1340

cross-section have the highest fundamental frequencies for the A and B geometries, while the prolate shells have the highest fundamental frequencies for the C and D geometries.

In Table 6, the DQM results for natural frequencies for isotropic toroidal shells of prolate elliptical cross-section with a line support at the inner equator are compared with FEM results. The material properties are those of Eq. (8). The agreement is within 1.7%, except for one value where there is a difference of 22%. The mode shapes corresponding to the six lowest natural frequencies of the shell cases C1, C2, C3, and C4, as determined by the FEM, are given in Figs. 2–5. The mode numbers indicated by the diagrams generally agree with the DQM mode numbers given in Tables 3–6. In this study it was observed that both the DQM and FEM may miss eigenvalues. This may arise due to inherent assumptions in the form of the solution, or due to problems in the extraction of the eigenvalues. Clearly, the simultaneous use of two methods is helpful in identifying a full set of modes.

### 6. Conclusions

A procedure has been outlined which enables the determination of the natural frequencies of orthotropic toroidal shells of elliptical cross-section. Comparison of results for isotropic toroidal shells of elliptical



cross-section and for orthotropic toroidal shells of circular cross-section show good agreement with previous results. New results given for toroidal shells of elliptical cross-section, without and with a circumferential line of support, show good agreement with finite element results.

## References

- [1] G. Yamada, Y. Kobayashi, Y. Ohta, S. Yokota, Free vibration of a toroidal shell with elliptical cross-section, *Journal of Sound and Vibration* 135 (1989) 411–425.
- [2] X.H. Wang, D. Redekop, Natural frequencies and mode shapes of an orthotropic thin shell of revolution, *Thin-Walled Structures* 43 (2005) 733–750.
- [3] W. Soedel, *Vibration of Shells and Plates*, third ed., Marcel Dekker, New York, 2004.
- [4] C. Shu, *Differential Quadrature and its Application in Engineering*, Springer, Berlin, 2000.
- [5] *ADINA Verification Manual*, ADINA R & D Inc., Watertown, 2003.